Materials Science & Engineering A 590 (2014) 37–43

Contents lists available at ScienceDirect

Materials Science & Engineering A

journal homepage: www.elsevier.com/locate/msea

A multiscale approach for the deformation mechanism in pearlite microstructure: Experimental measurements of strain distribution using a novel technique of precision markers

Masaki Tanaka [a,*], Yusuke Yoshimi [a], Kenji Higashida [a], Tomotsugu Shimokawa [b], Tetsuya Ohashi [c]

[a] Department of Materials Science and Engineering, Kyushu University, 744 Motooka, Nishi-ku, Fukuoka 819-0395, Japan
[b] School of Mechanical Engineering, Kanazawa University, Kakuma-machi, Kanazawa, Ishikawa 920-1192, Japan
[c] Kitami Institute of Technology, 165 Koencho, Kitami 090-8507, Japan

ARTICLE INFO

Article history:
Received 11 August 2013
Accepted 20 September 2013
Available online 8 October 2013

Keywords:
Steels
Local deformation
High-precision markers
Wire drawing

ABSTRACT

Plastic deformation of fully pearlitic steels was investigated using a multiscale approach: experimentally, the finite element method and molecular dynamics. This paper is the first in a series of three papers demonstrating the strain distribution in uniaxial tensile deformation with high-precision markers drawn by electron beam lithography. Strain was measured at loads of 1.98 kN, 2.21 kN and 2.28 kN in tensile deformation. Scanning electron microscopy (SEM) images and strain maps show the plastic deformation of cementite lamellae and homogenous plastic deformation under uniaxial tensile deformation in the area where the cementite lamellae are aligned in the tensile direction. The areas where strain was enhanced were both block/colony boundaries and the areas where the cementite lamellae are inclined approximately 45° to the tensile direction.

1. Introduction

Pearlitic steels consist of cementite and ferrite that form lamellar structures. Single-phase cementite is brittle at room temperature, whereas it becomes ductile at high temperatures [1,2]. The combined structure with such brittle and ductile phases in steels induces interesting mechanical properties. For example, the yield stress of pearlitic steels is an inverse function of the interlamellar spacing and their ductility depends on the size of the blocks [3,4]. It is also reported that pearlitic steels show good work-hardening ability. Using neutron diffraction, Tomota et al. [5] elucidated that such significant work hardening is due to stress partitioning between the ferrite and cementite, where internal stresses induced by the misfit of plastic strain between the two phases cause high and low stress states in the cementite and ferrite phases, respectively. However, the fundamental deformation process of pearlitic steels has not been fully elucidated yet, particularly the characteristics of inhomogeneous plastic deformation of ferrite and cementite lamellae. It is essential to elucidate how the plastic deformation of pearlitic steels depends on the direction of the pearlite lamellae, colonies and blocks. In addition, it has not been clarified yet whether cementite lamellae can be plastically elongated in tensile deformation at room temperature, whereas it has been reported that they deform under cold rolling [6] or wire drawing [7]. One of the difficulties in investigating whether or not cementite lamellae can plastically deform during uniaxial tensile deformation is that cementite lamellae are not innately straight [8] and are fragmented [9]. Therefore, it is not straightforward to determine whether the observed cementite lamellae were deformed during tensile tests [8]. Thus, it is essential to observe and compare the same area in order to investigate plastic deformation of the cementite lamellae under the uniaxial tensile deformation.

In the present paper, the plastic strain distribution during tensile deformation was investigated in fully pearlitic steels using high-precision markers drawn on the specimen surface by electron beam lithography. In addition, the characteristics of the inhomogeneous deformation of pearlitic steels were also observed using backscattered electrons (BSE) with an angle-selected backscattered electron detector. The purpose of the present paper is to show experimentally the inhomogeneous behaviour of plastic deformation in pearlitic steels. The strain in the pearlitic steels and cementite lamellae were quantitatively measured for the first time. The results correlate with the modelling and simulation studies on the mechanical behaviours of this kind of characteristic lamellar structure reported in separate papers [10,11].

2. Experimental procedures

Tensile specimens were cut from a 5.5 mm diameter patented SWRS92A fully pearlitic steel, as shown in Fig. 1(a). The crosshead

* Corresponding author. Tel./fax: +81 92 802 2973.
E-mail address: masaki@zaiko.kyushu-u.ac.jp (M. Tanaka).

0921-5093/$ - see front matter
http://dx.doi.org/10.1016/j.msea.2013.09.072

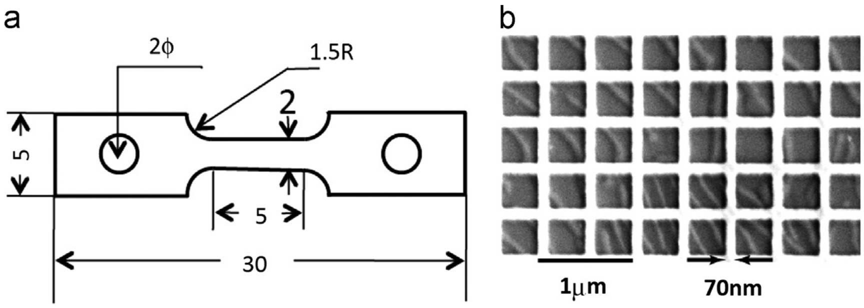

Fig. 1. (a) Schematic drawing of the tensile specimen. The specimen thickness was 1 mm. The specimen was cut from the centre of a 5.5 mm diameter bar. (b) SEM image from the undeformed surface showing the 0.5 μm square high-precision markers. The width of each marker was approximately 70 nm.

speed in the tensile test was set to be 0.2 mm/min (Shimazu: AG-IS). The average block size and interlamellar spacing of the samples were 20 μm and 150 nm, respectively. In order to elucidate the distribution of strain in the specimen, precision markers were first drawn on the parallel portion of the specimen surface using electron lithography [12,13]. The shape of the precise markers was a square with one side being 500 nm in length, as shown in Fig. 1(b). The width of the markers was approximately 70 nm. Strain was measured from the displacement of the vertices of the square. Precise coordinates were put on each vertex of the square lattice in the scanning electron microscope (SEM) images before deformation, and then we measured the relative displacement of each coordinate in the x and y directions (parallel and perpendicular to the tensile direction) after deformation. The BSE images were obtained using an angle-selected backscattered electron detector in an SEM (Carl Zeiss: Ultra-55).

The strain in each square was evaluated as follows. First, each square was divided into four triangles by connecting two vertices on a diagonal line. We selected one triangle and assumed that any point inside the triangle, given as (x^i, y^i), before deformation moved of (u^i, v^i), after deformation. We regard the linear relationship between them, such that

$$u^i = a + bx^i + cy^i, \tag{1}$$

$$v^i = d + ex^i + fy^i, \tag{2}$$

where a, b, c, d, e and f are the real numbers. Here, the coordinates of the vertices of one of the triangles before and after deformation were defined as (x_0^1, y_0^1), (x_0^2, y_0^2), (x_0^3, y_0^3) and (x^1, y^1), (x^2, y^2), (x^3, y^3), respectively. The displacement components of each vertex were

$$u^1 = x^1 - x_0^1, \quad v^1 = y^1 - y_0^1 \tag{3}$$

$$u^2 = x^2 - x_0^2, \quad v^2 = y^2 - y_0^2, \tag{4}$$

$$u^3 = x^3 - x_0^3, \quad v^3 = y^3 - y_0^3, \tag{5}$$

substituting Eqs. (3)–(5) into Eqs. (1) and (2) gives the values for a, b, c, d, e and f. The Green–Lagrange strain in two-dimension is given by the differential forms of Eqs. (1) and (2):

$$\varepsilon_{xx} = \frac{\partial u^i}{\partial x} + \frac{1}{2}\left(\frac{\partial u^i}{\partial x}\frac{\partial u^i}{\partial x} + \frac{\partial v^i}{\partial x}\frac{\partial v^i}{\partial x}\right), \tag{6}$$

$$\varepsilon_{yy} = \frac{\partial v^i}{\partial y} + \frac{1}{2}\left(\frac{\partial u^i}{\partial y}\frac{\partial u^i}{\partial y} + \frac{\partial v^i}{\partial y}\frac{\partial v^i}{\partial y}\right), \tag{7}$$

$$\gamma_{xy} = \frac{1}{2}\left(\frac{\partial u^i}{\partial y} + \frac{\partial v^i}{\partial x}\right) + \frac{1}{2}\left(\frac{\partial u^i}{\partial x}\frac{\partial u^i}{\partial y} + \frac{\partial v^i}{\partial x}\frac{\partial v^i}{\partial y}\right), \tag{8}$$

$$\varepsilon_{eq} = \sqrt{\tfrac{4}{3}(\varepsilon_x^2 + \varepsilon_x\varepsilon_y + \varepsilon_y^2) + \tfrac{1}{3}\gamma_{xy}^2}, \tag{9}$$

where ε_i $(i = xx,\ yy)$, γ_{xy} and ε_{eq} are the average of the total normal strain, the shear strain and the equivalent strain of each triangle after unloading, respectively. The strain of each square is the average value of the strain from all four triangles in the square.

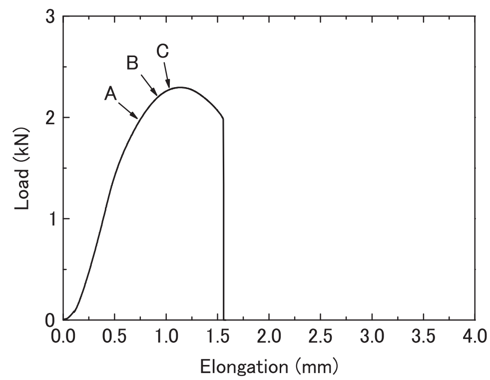

Fig. 2. Load–elongation curve of fully pearlitic steel using the specimen in Fig. 1. Crosshead speed was set to be 0.2 mm/min. The curve includes the stiffness of the tensile machine used. The values of strain were measured at A, B and C at loads of 1.98 kN, 2.21 kN and 2.28 kN, respectively.

3. Results and discussion

3.1. Strain distribution during uniaxial tensile deformation

Fig. 2 shows a load–elongation curve in a tensile test, which includes the stiffness of the tensile test machine. The fully pearlitic steel shows significant work hardening just after yielding, which is due to the stress partitioning between the cementite and ferrite phases [14]. Another tensile test was performed using a different specimen from that used in Fig. 2. The applied load was terminated and unloaded at loads of 1.98 kN, 2.21 kN and 2.28 kN. The strain distribution was measured from the deviation of the vertices of the markers on the specimen surface.

Fig. 3(a), (b) and (c) shows equivalent strain maps in which the tensile tests terminated and unloaded at loads of 1.98 kN, 2.21 kN and 2.28 kN, respectively. The tensile direction was horizontal in the figure. The measured area was approximately $100 \times 50\ \mu m^2$. Histograms of the equivalent strain from Fig. 3(a), (b) and (c) are shown in Fig. 3(d), (e) and (f), respectively. The statistical data are shown in Table 1. The lognormal fit curves are superposed upon each histogram of strain in Fig. 3(d)–(f), exhibiting shapes of strain distribution that are close to those of the lognormal distribution. These results indicate that the values of the strain median are smaller than the strain average, showing that a small number of areas with large strains contributed to the increase in the average of the strain. It also indicates that the increase in the strain in fully pearlitic steels is a multiplicative process. The strain maps indicate inhomogeneous plastic deformation of the specimen. Fig. 3(a)–(c)